SAND2015-3767C

Exceptional service in the national interest

Sandia National Laboratories

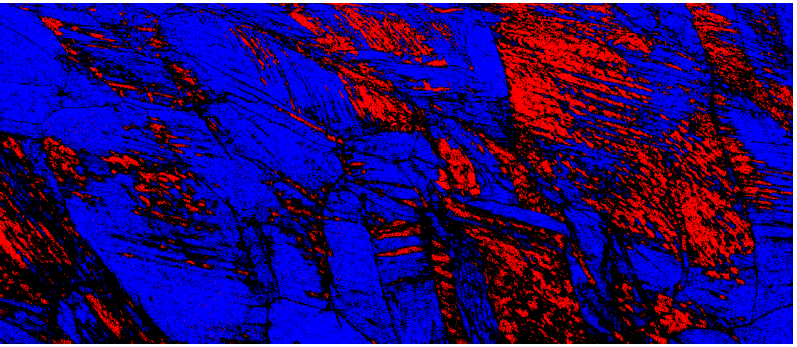
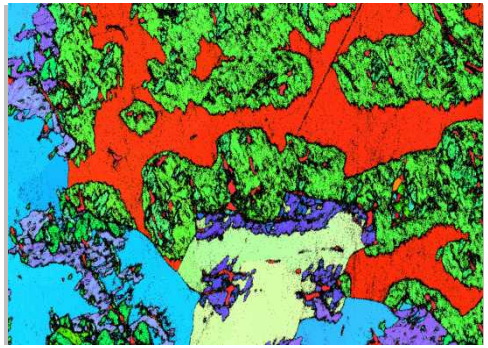
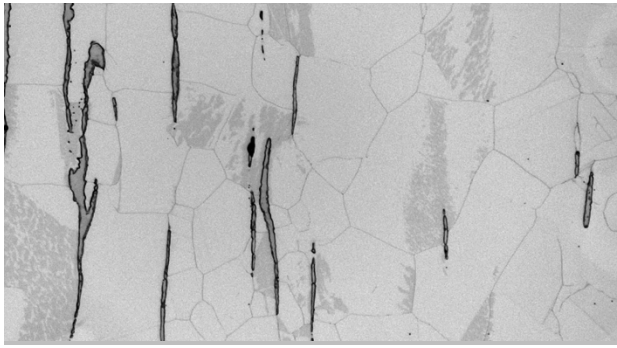

Artifact-Free Determination of Weld Metal Constitution in Austenitic Stainless Steels

J. M. Rodelas, M.C. Maguire, J.R. Michael

Sandia National Laboratories, Albuquerque NM

May 12th, 2015

U.S. DEPARTMENT OF ENERGY | NNSA National Nuclear Security Administration

Sandia National Laboratories is a multi-program laboratory managed and operated by Sandia Corporation, a wholly owned subsidiary of Lockheed Martin Corporation, for the U.S. Department of Energy's National Nuclear Security Administration under contract DE-AC04-94AL85000. SAND NO. 2011-XXXXP

Austenitic Stainless Steel Background

- Austenitic stainless steels are based on the Fe-Cr-Ni system
- Extensive use in Sandia components (304L)
  - Excellent corrosion resistance
  - Excellent ductility
  - Strength comparable to mild steel
  - *Weldable**





- Microstructural constitution ranges from single phase to triplex

A: Austenite

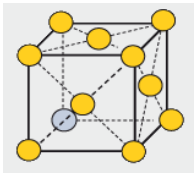

fcc: face-centered cubic

F: Ferrite

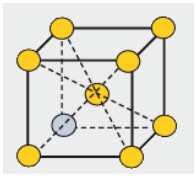

bcc: body-centered cubic

Martensite

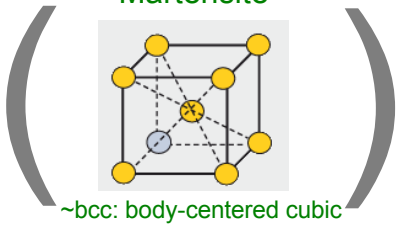

~bcc: body-centered cubic

- 16 - 25 Chromium
- 8 - 20 Nickel
- 1 - 2 Manganese
- 0.5 - 3 Silicon

- 0.02 - 0.1 Carbon
- 0 - 2 Molybdenum
- 0 - 0.15 Nitrogen
- 0 – 2 Titanium or Niobium

Ferrite Plays Important Role in Austenitic Stainless Steel Welds

- Ferrite in an austenitic stainless weld influences:
  - Weldability
  - Mechanical response
  - Environmental cracking susceptibility
  - Cryogenic & elevated temperature properties

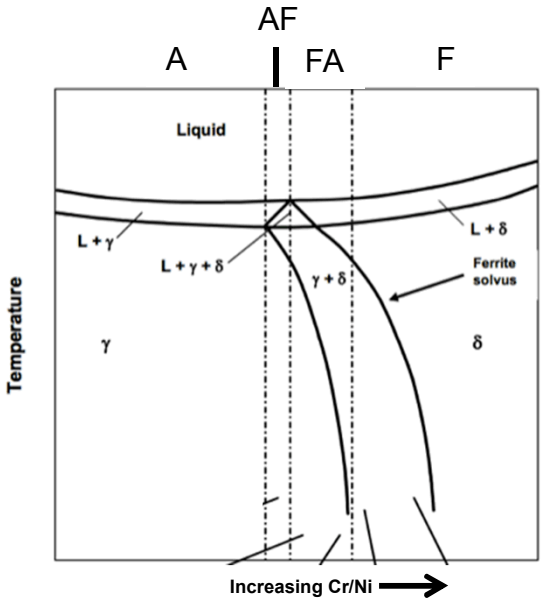

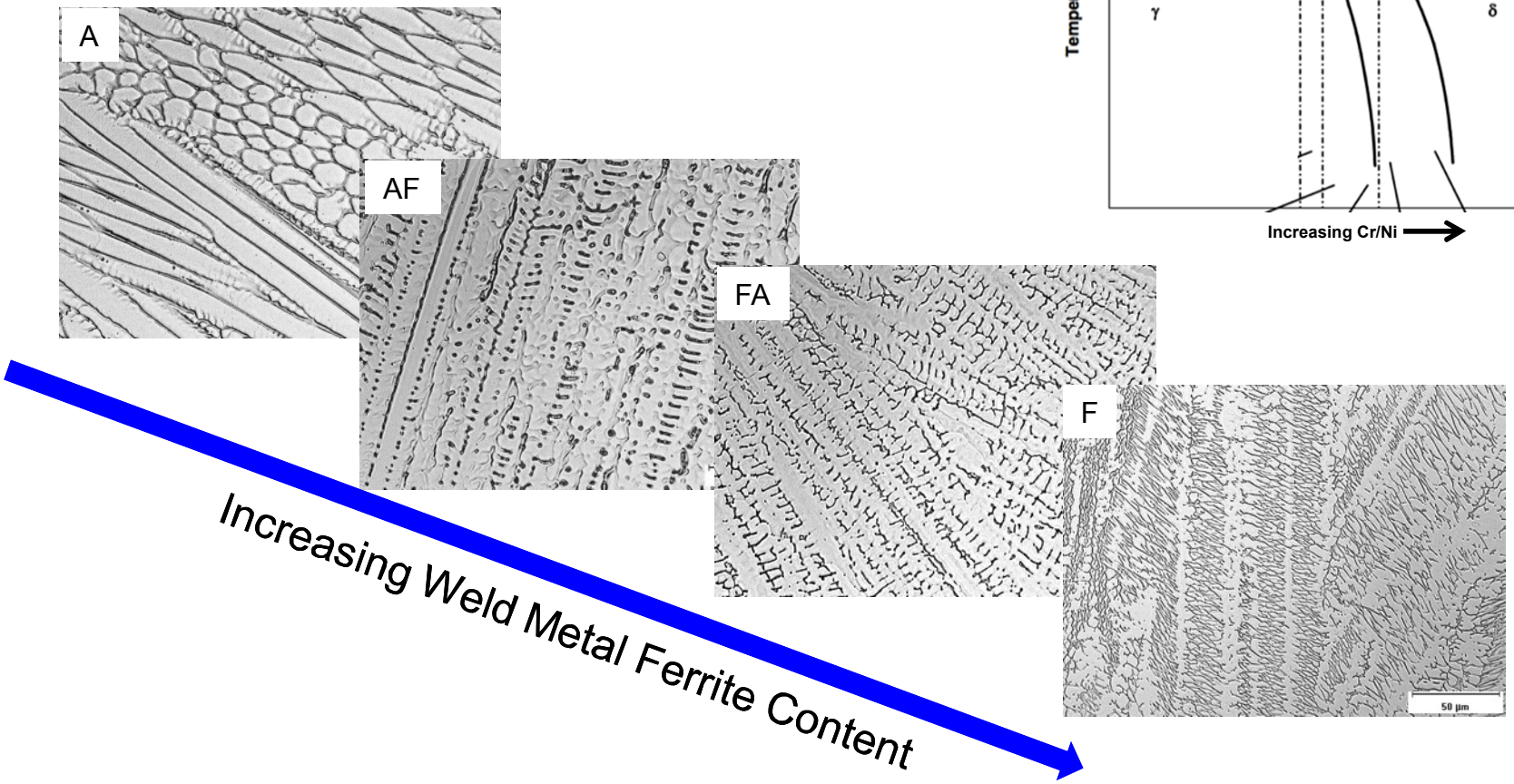

Understanding Austenitic Stainless Steel Weld Mechanical Behavior Variation Requires Accurate Knowledge of Phase Distribution

- 60-70% of mechanical behavior variation attributed to non-metallurgical factors (e.g., weld shape, joint geo., etc.)

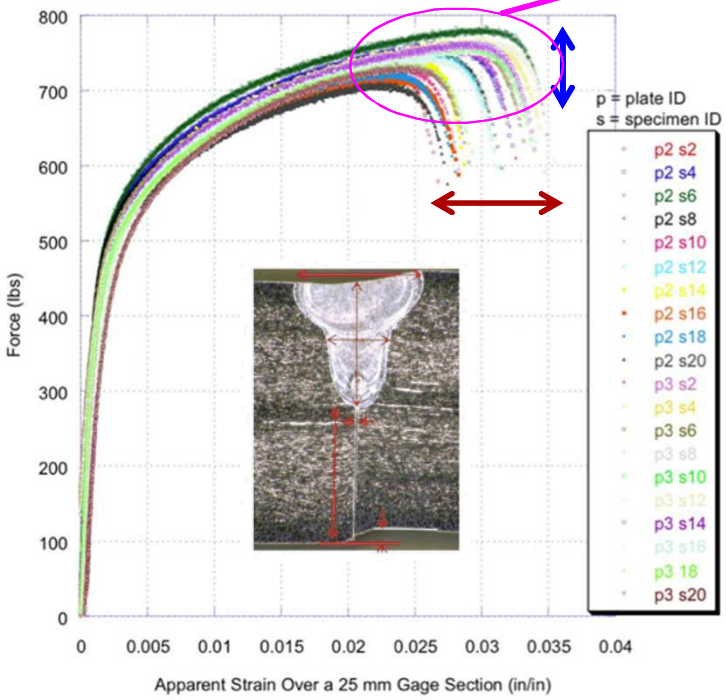

- Characterization of property variation due to metallurgical factors requires accurate characterization of phase constitution

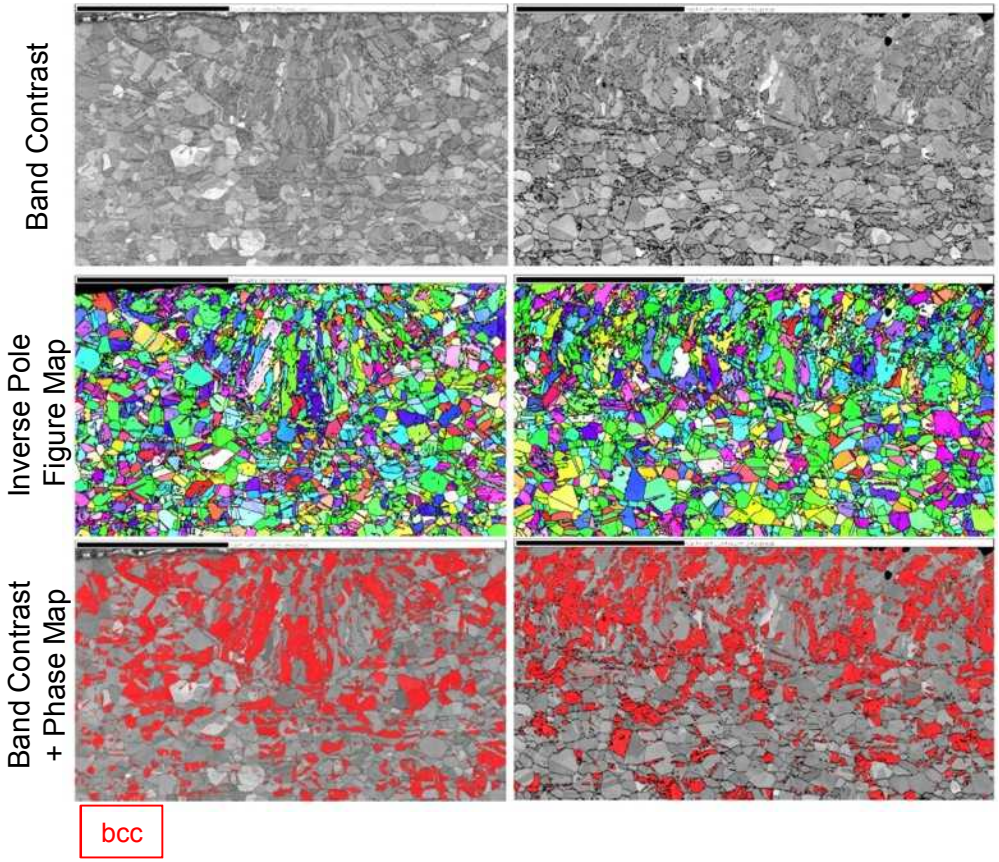

Metallographic Preparation for EBSD Phase Distribution Requires Additional Scrutiny

Sandia National Laboratories

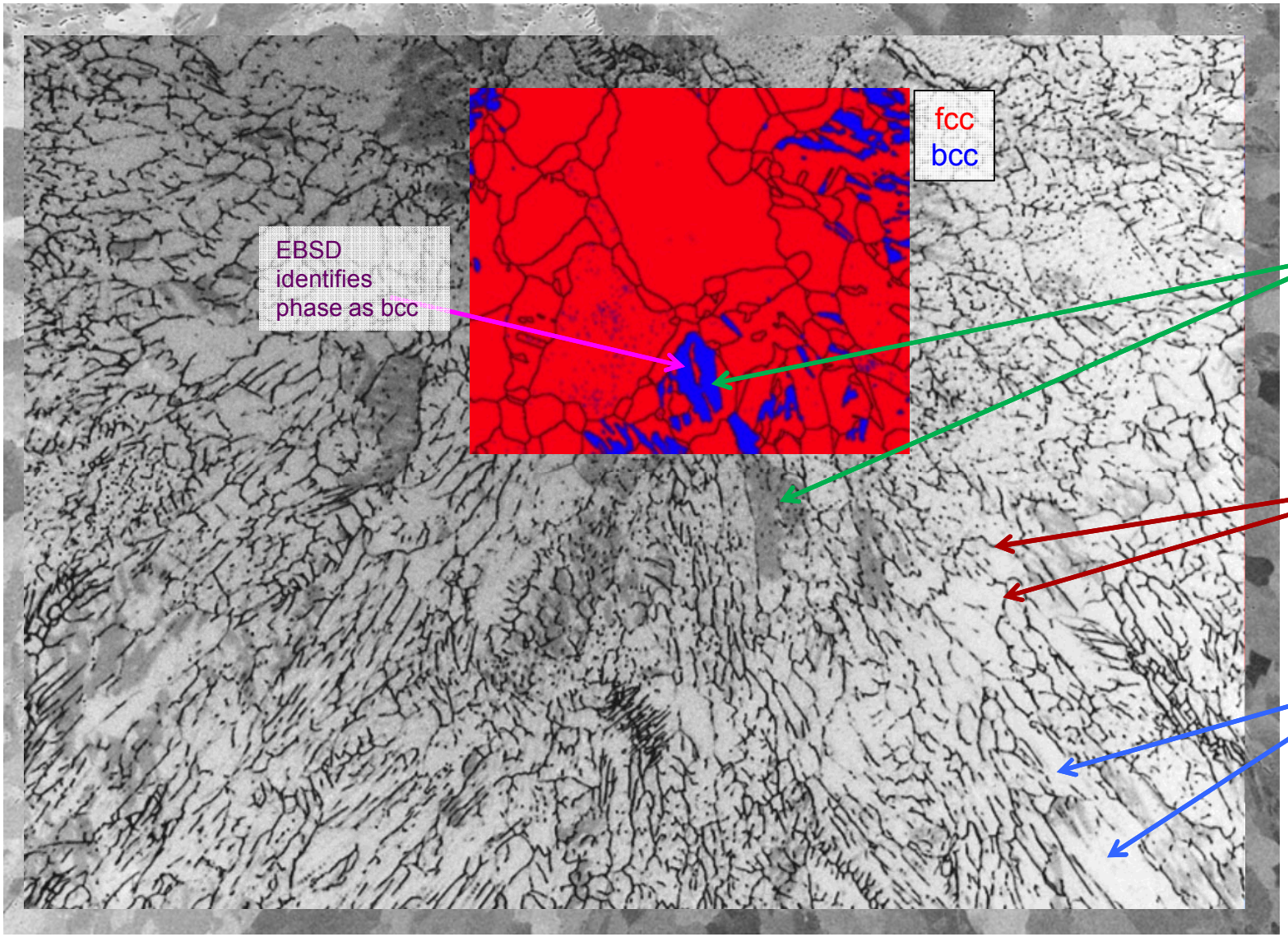

304L laser weld mechanically polished using conventional metallographic practices

Additional Martensite Examples: Preparation-Induced

Odegard, B.C. Metallography, 7, 129-135 (1974)

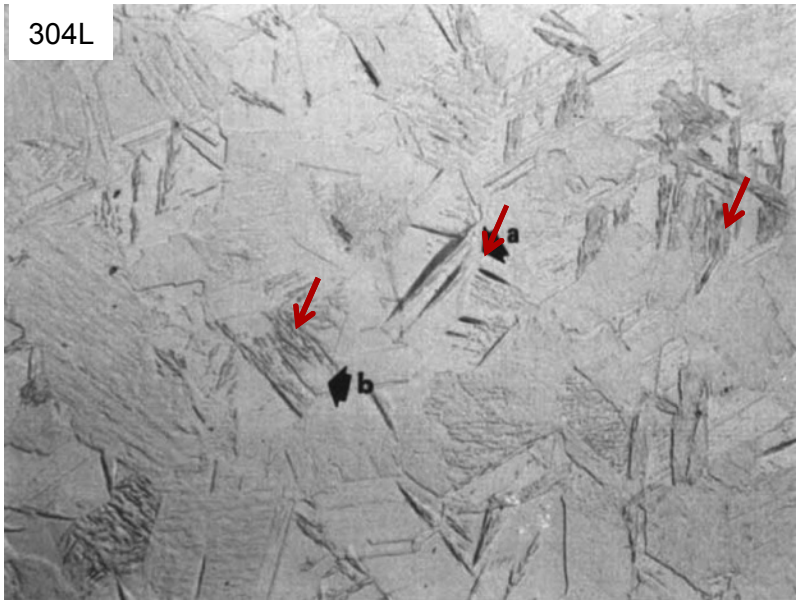

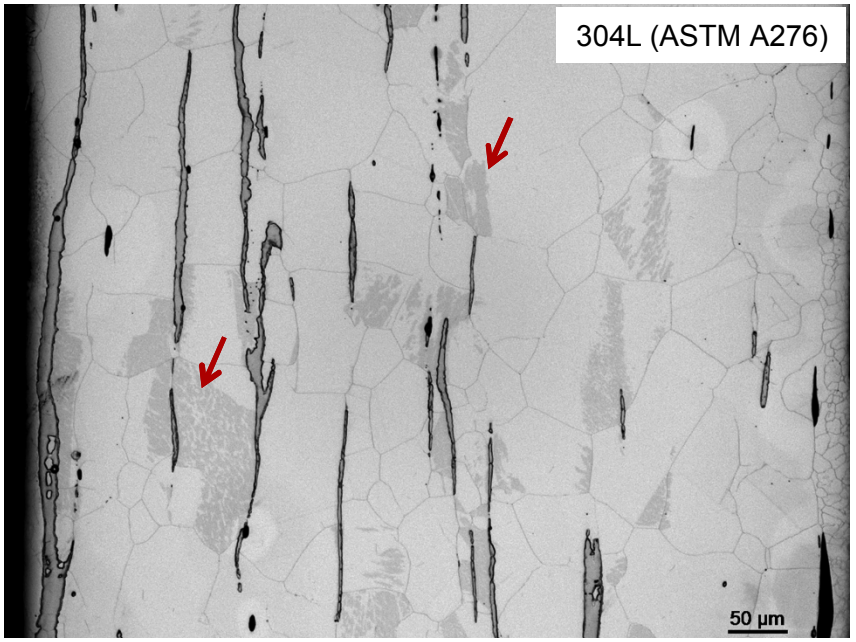

Pascal, C., et al. Corrosion Science, 93, 100-108 (2015)

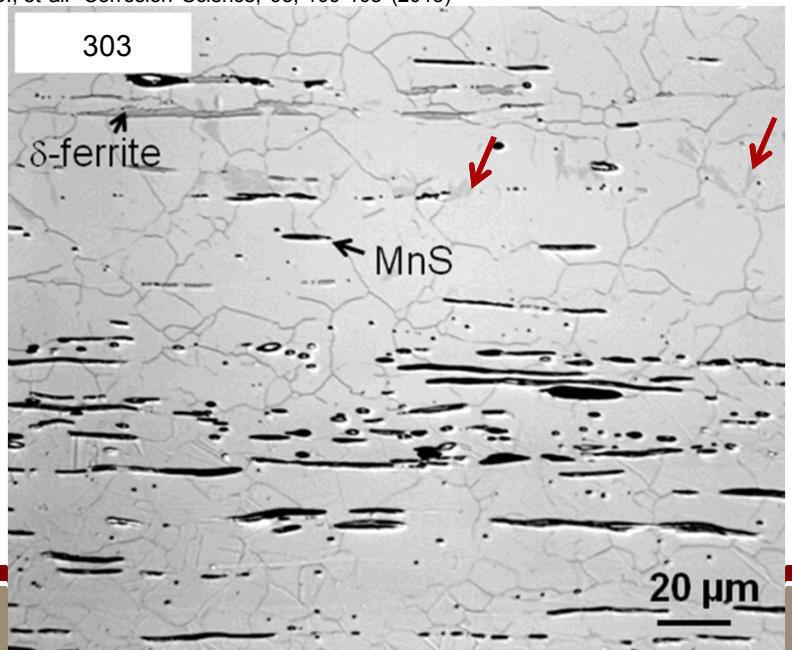

Electropolishing Eliminates Ambiguity in EBSD Ferrite Determination

Band Contrast + Phase Map: bcc

Mechanically Polished

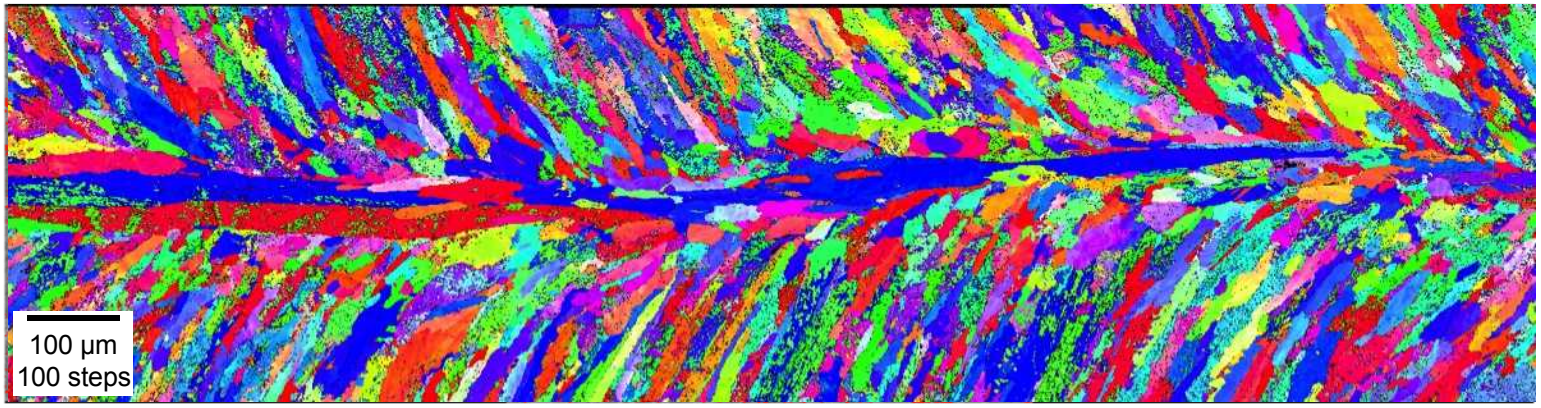

Electropolished

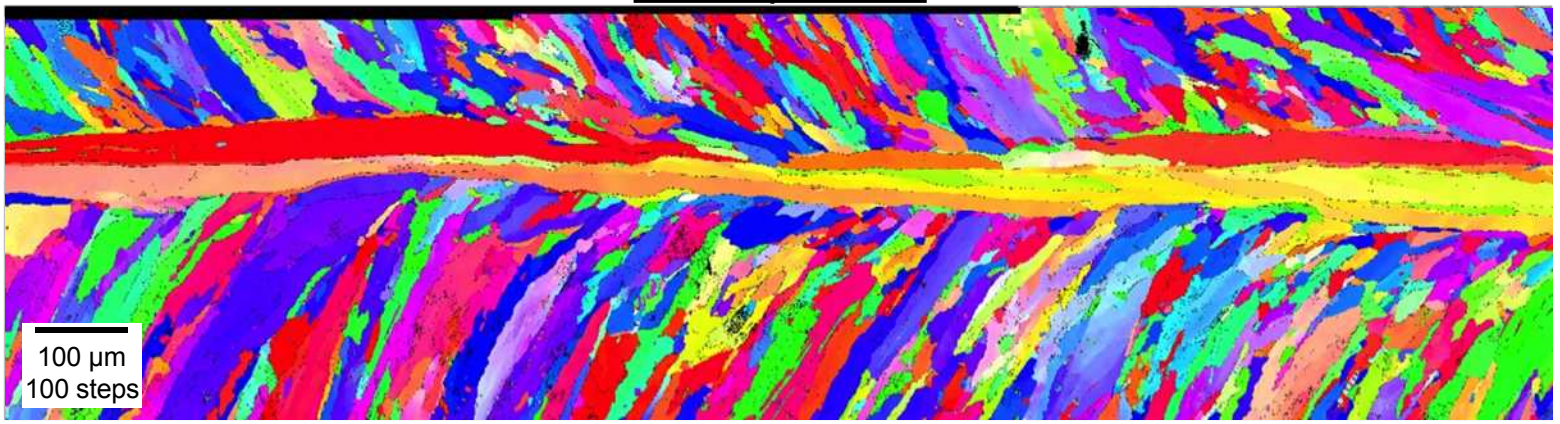

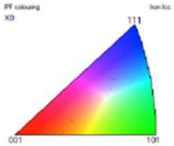

80 vol% H_3PO_4 + 20 vol% n-Butanol @ 70ºC, 1 A/cm^2

Welding Direction

Continuous Wave Nd:YAG Laser Weld on 304L

Preparation-Induced Martensite: Effect of Preparation Technique

Sandia National Laboratories

- Preparation-induced martensite not eliminated by reducing grinding/polishing downforce

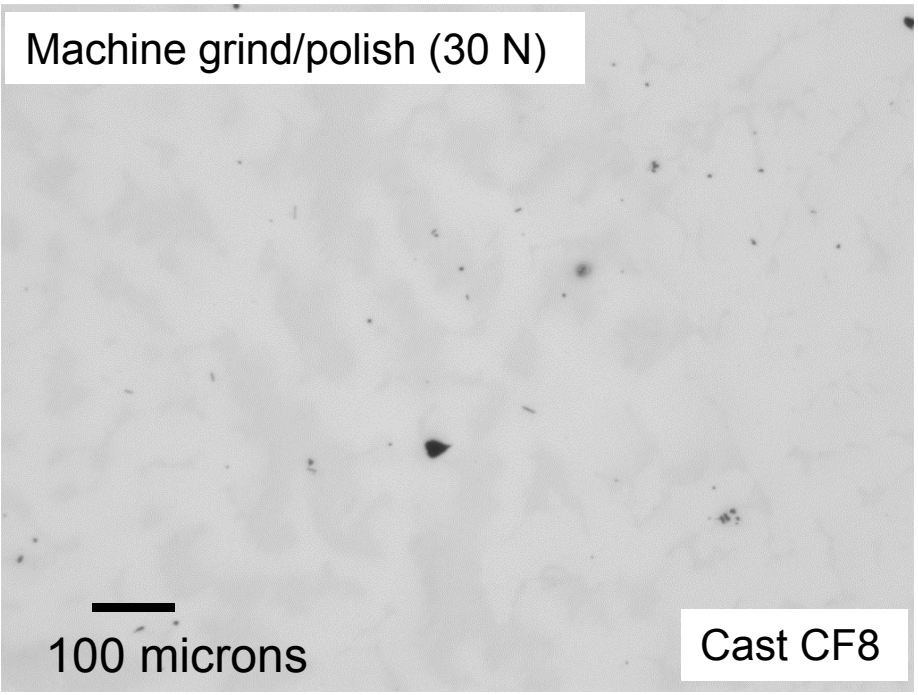

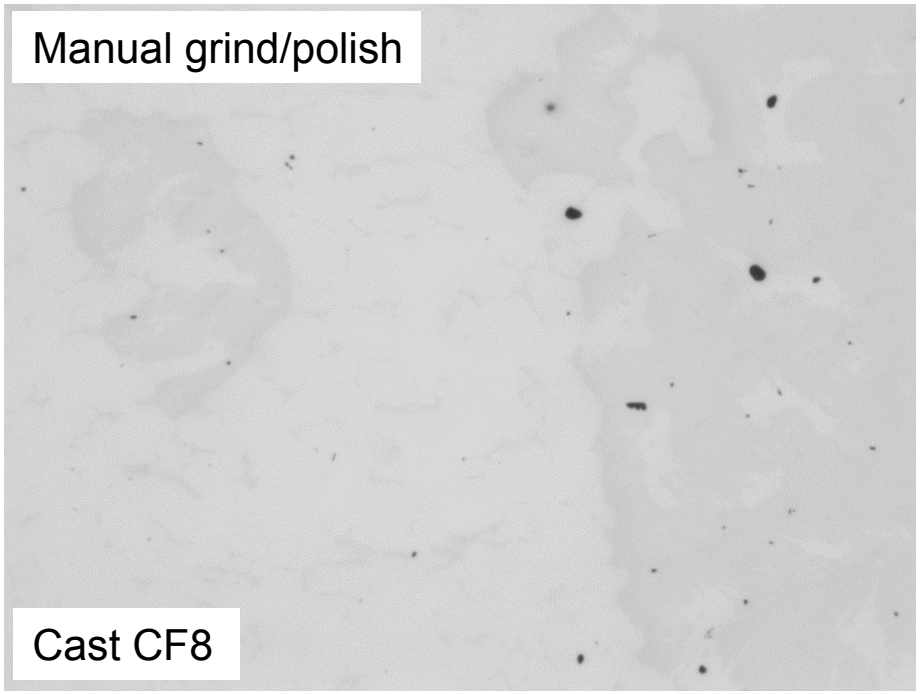

- Section sample via abrasive saw
- Grind using SiC or Al_2O_3 papers through 600 grit
- Diamond polish 9 → 6 → 3 → 1 µm
- Vibratory polish 0.3 µm Al_2O_3 followed by 0.04 µm SiO_2

304L Shear Test Specimens Show Deformation-Induced Martensite

- Controlled shear loading of commercial wrought 304L leads to room-temperature deformation-induced martensite

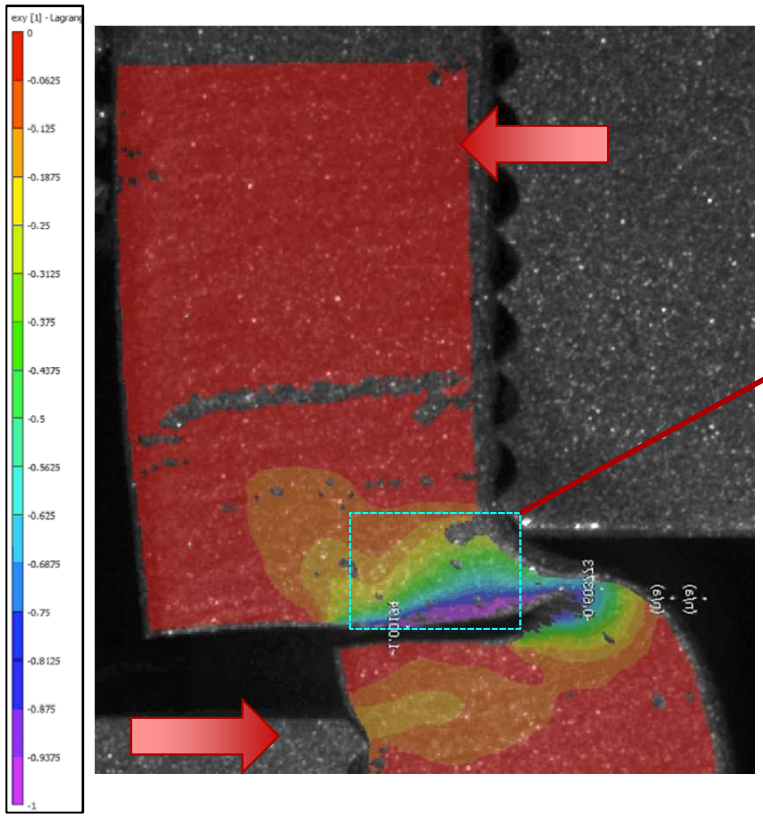

Optical micrograph of shear specimen (*electropolished*)

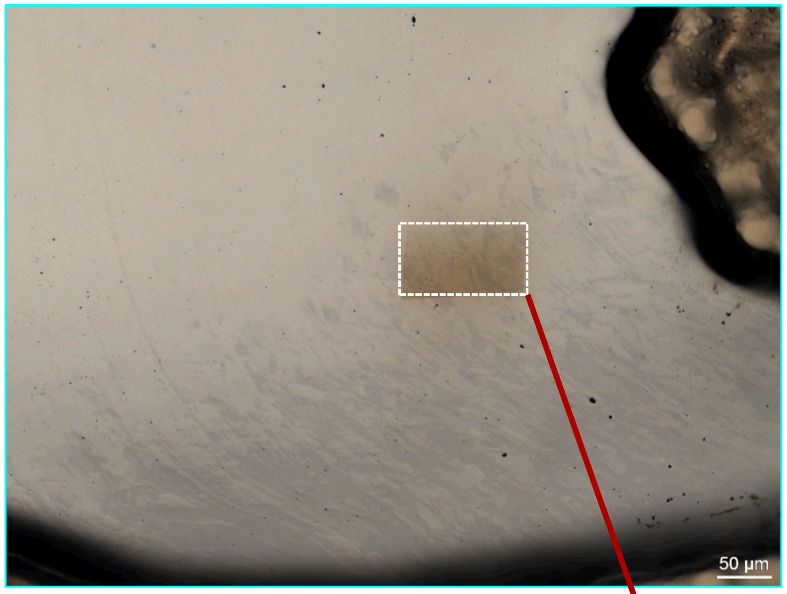

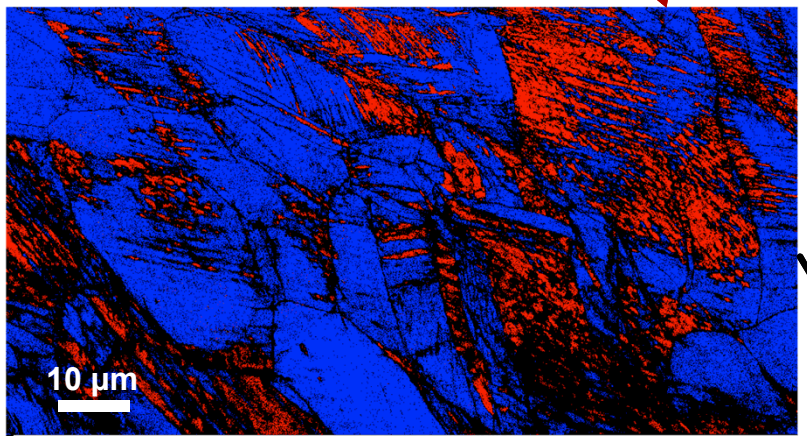

Phase Map: **fcc**; **bcc**

- Increasing Shear Strain
- Decreasing Diffraction Indexing Accuracy
- Increasing Martensite Fraction

Solidification Microstructures More Sensitive to Strain-Induced Transformation

- Martensite (formed by mechanical polishing) preferentially forms around certain regions in solidification microstructure

Autogenous LBW plan view section of laser weld (*mechanically polished*)

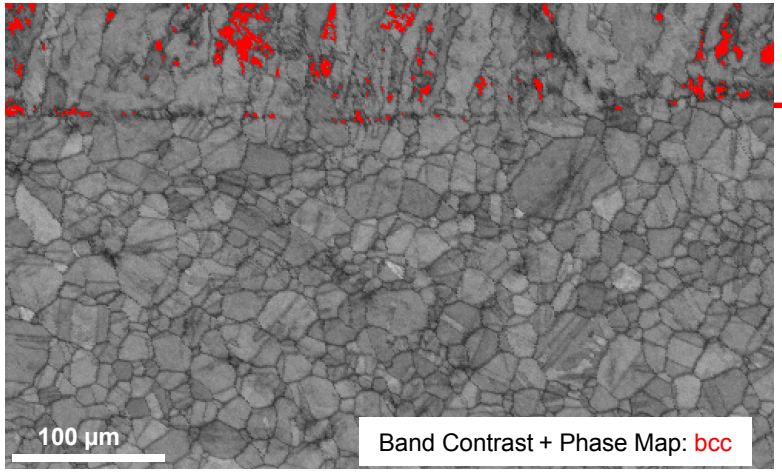

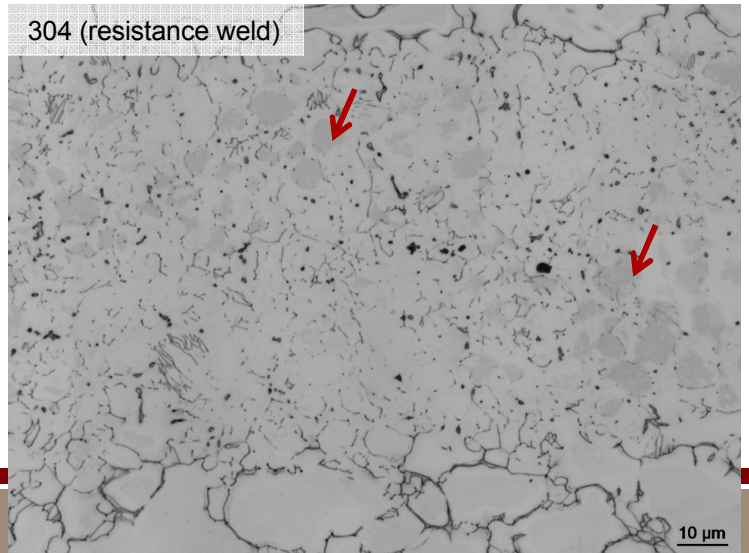

Cast CF8 stainless (*mechanically polished*)

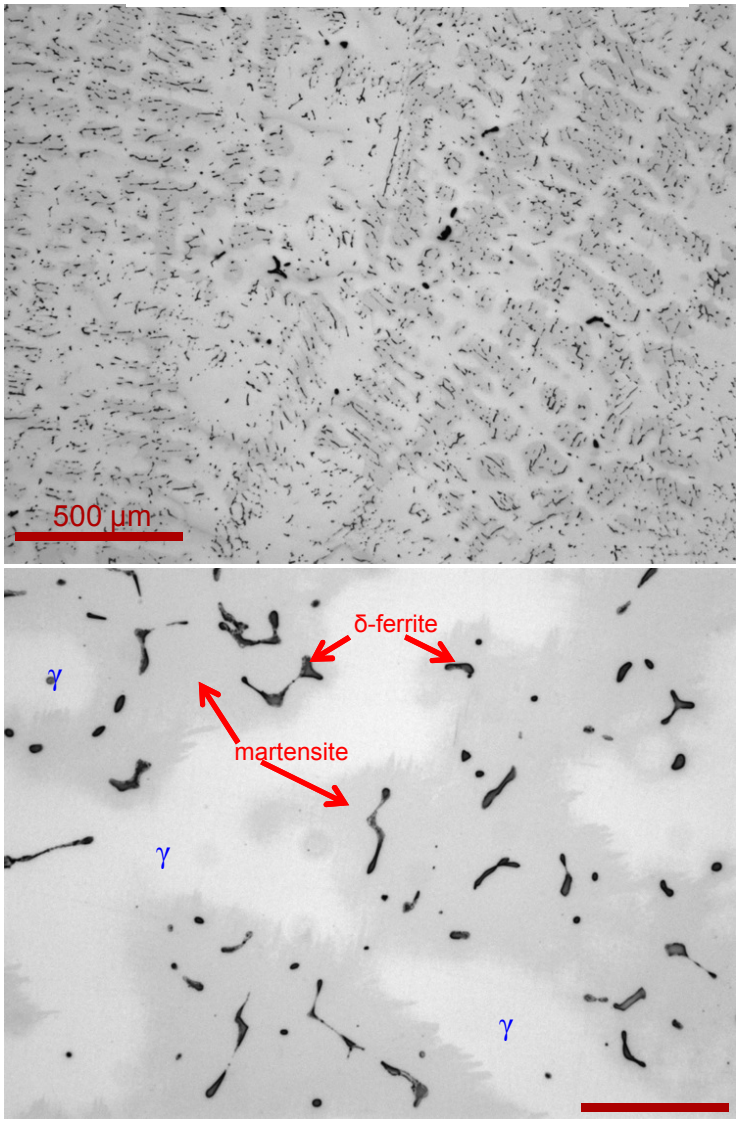

- Light etch (electrolytic NaOH) to stain δ-ferrite

EBSD Analysis Confirms Martensite Formation in CF8

Sandia National Laboratories

Phase Map: **bcc**; **fcc**

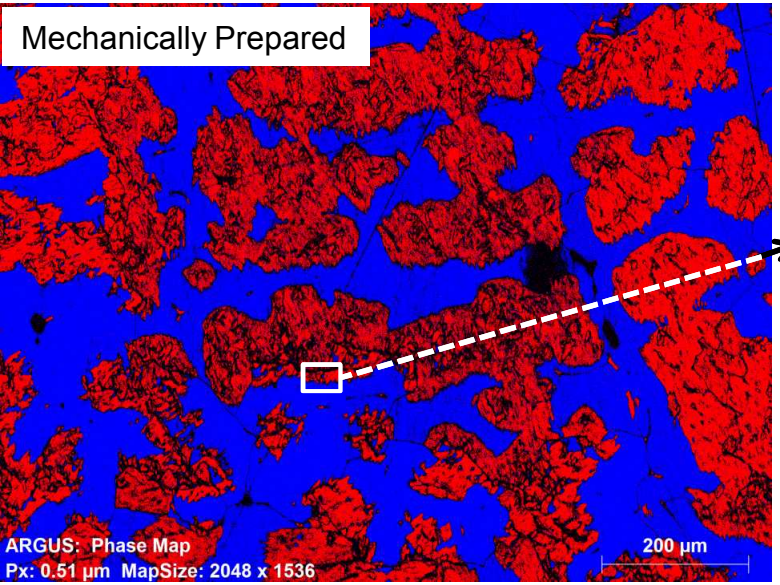

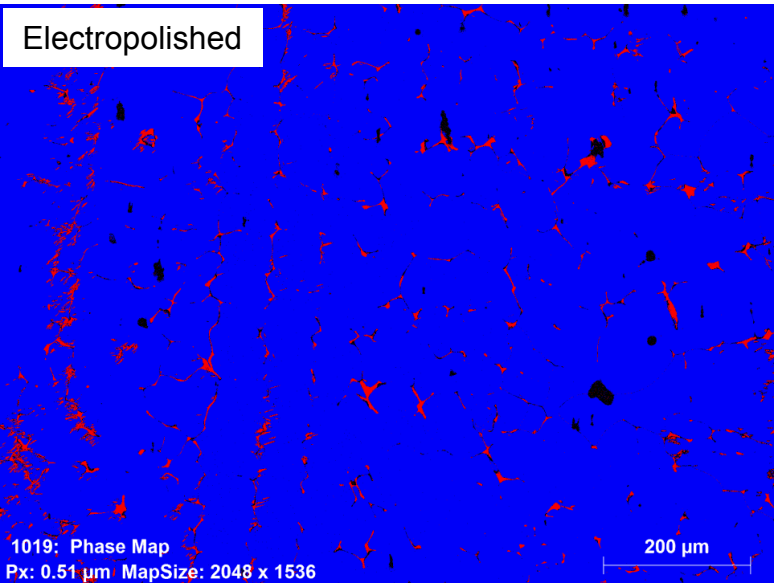

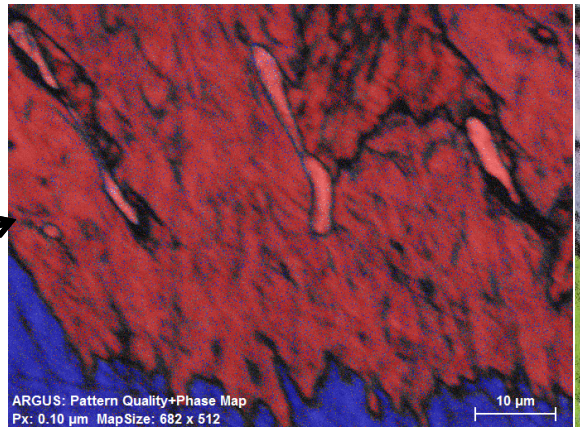

Phase Map: bcc; fcc

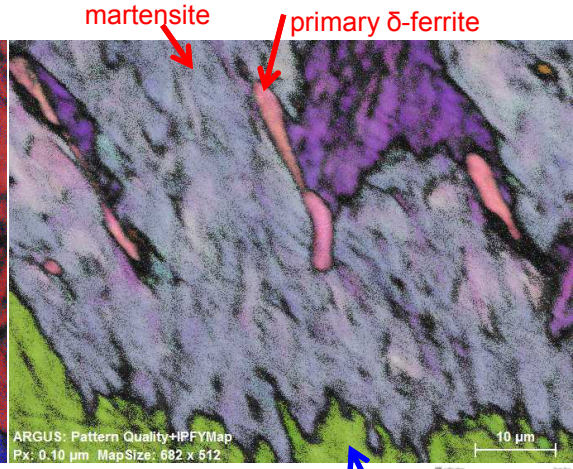

IPF-Y

- Intermediate gray phase observed in optical micrographs indexed as bcc phase
- EBSD measurements of mechanically polished cast 304 produces highly erroneous measurements of residual δ-ferrite
- *Why do solidification microstructures tend to have increased propensity to local deformation-induced martensite?*

Role of Elemental Partitioning During Solidification Examined

- During solidification, elemental segregation results in an heterogeneous local distribution of alloying elements– especially within initial and final transient regions

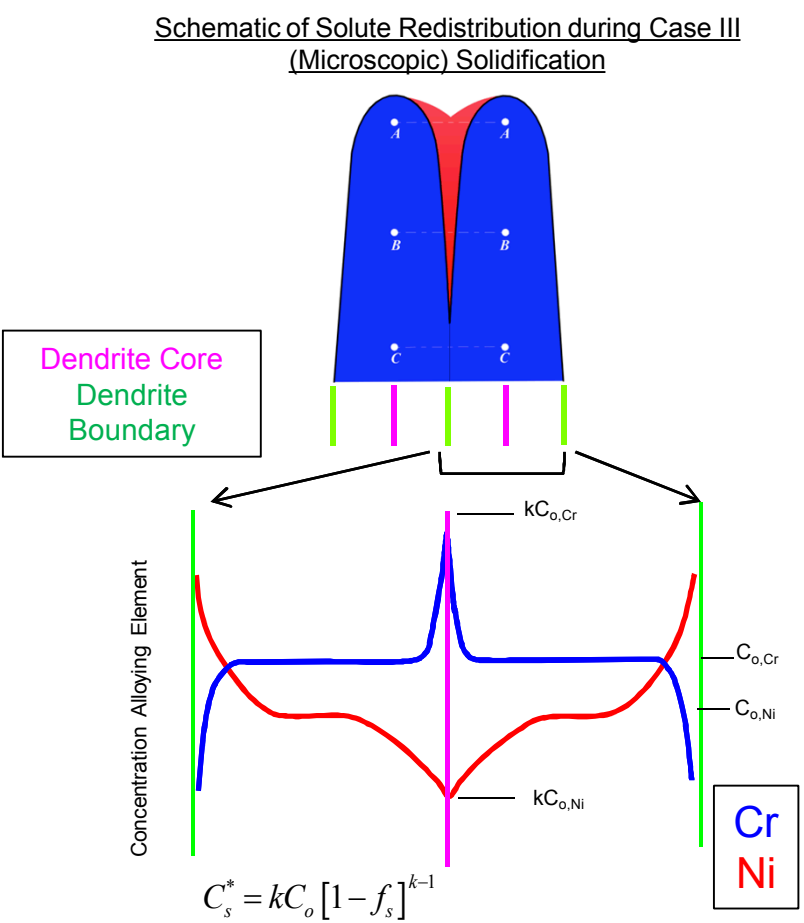

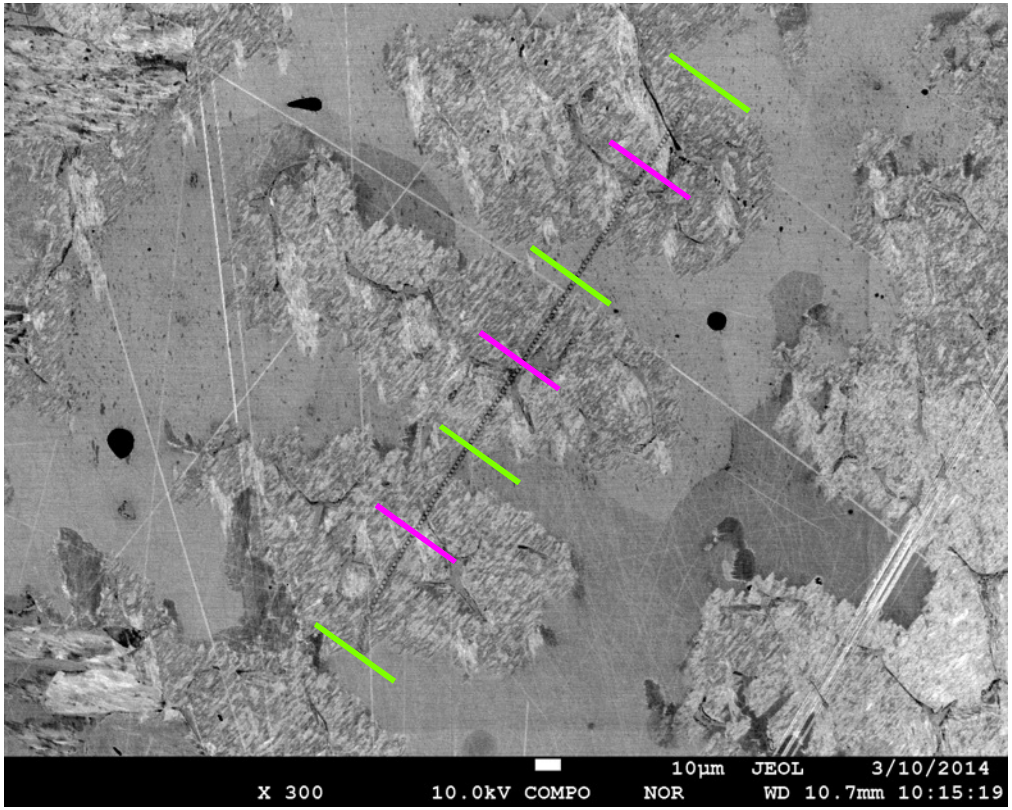

Backscatter electron micrograph of cast CF8 stainless steel solidifying as primary ferrite

Role of Elemental Partitioning During Solidification Examined

- Elemental partitioning behavior is consistent with solidification of casting (primary-ferrite)
- Coarse solidification microstructure allows phase identification from backscatter channeling contrast imaging in conjunction with WDS microprobe

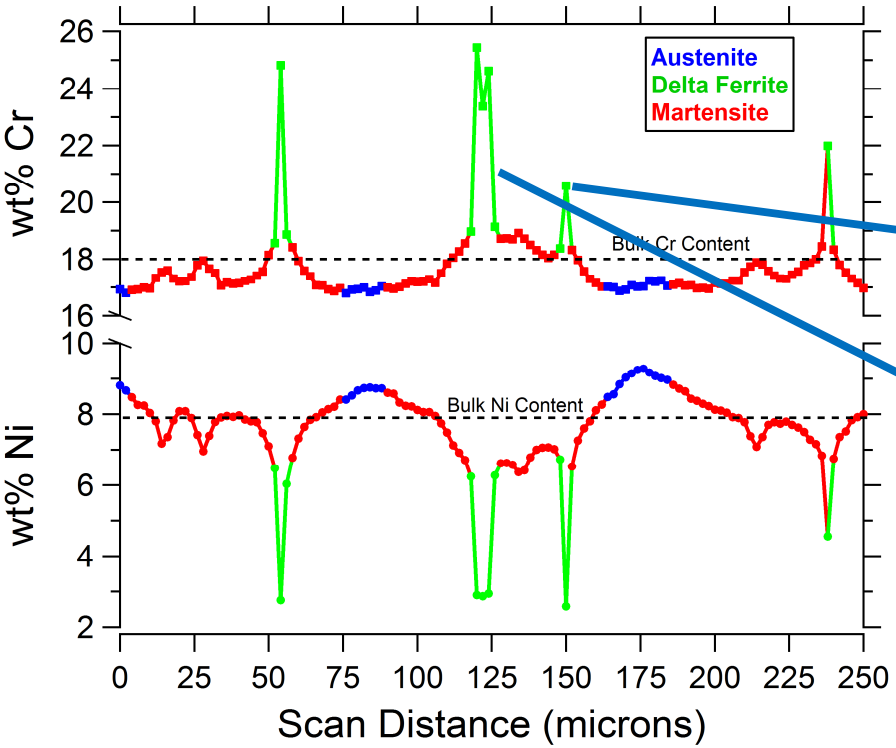

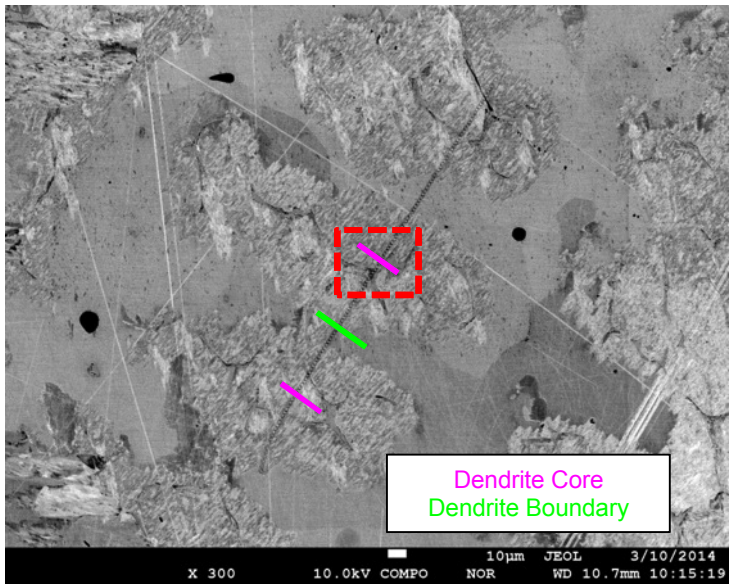

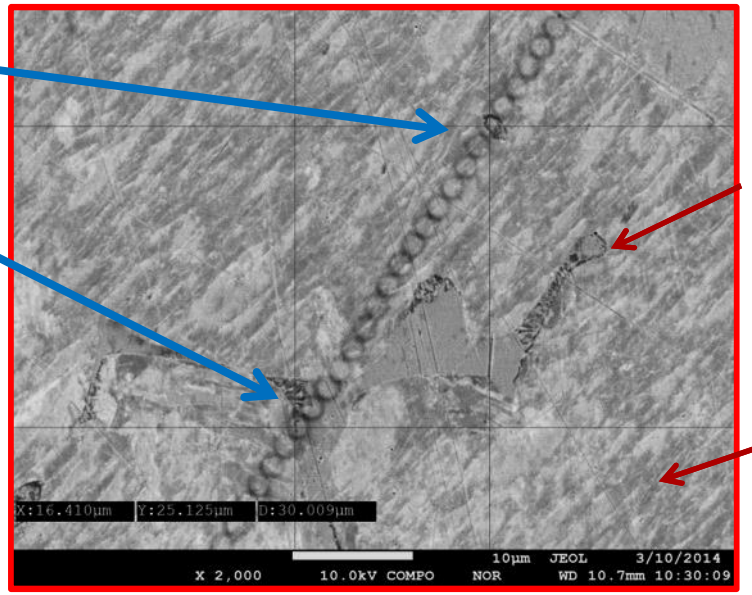

Elemental Mapping of Chemical Segregation Reveals Distribution of Deformation-Induced Martensite Sensitivity

Sandia National Laboratories

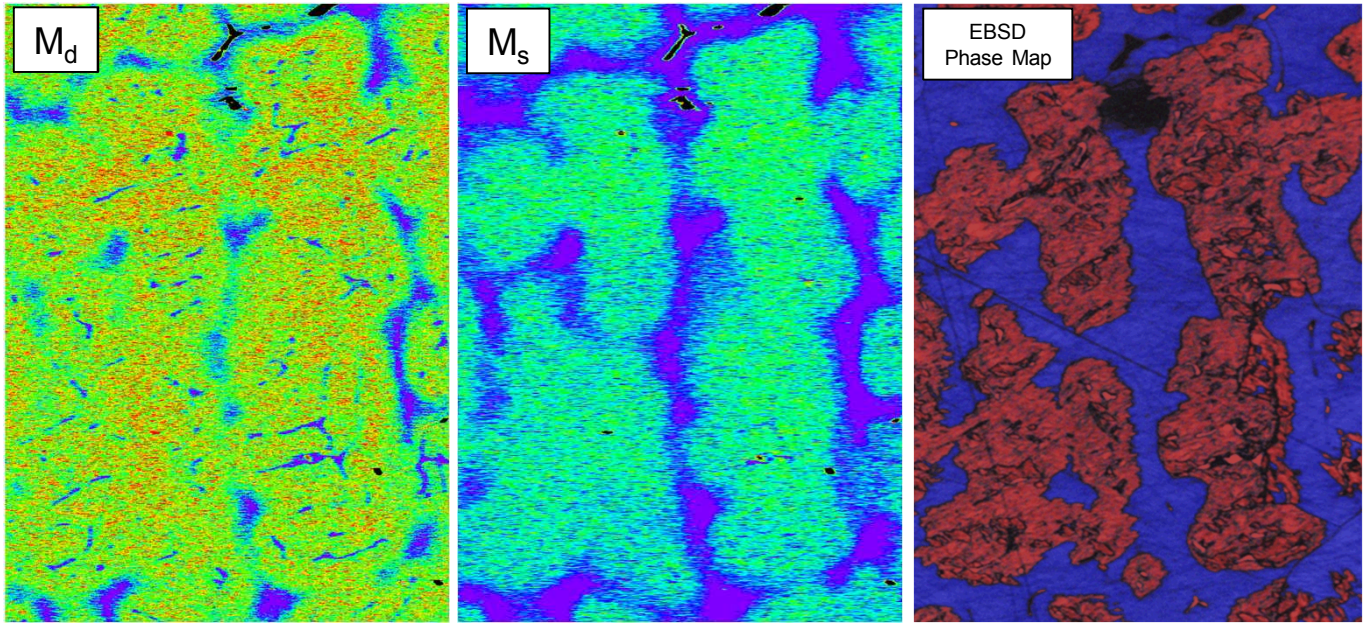

- Relative differences in chemical driving force for austenite instability can be easily visualized in chemically heterogeneous solidification microstructures

M_s & M_d maps generated from measured composition (assumes bulk C & N concentration)

Angel et al. (1954)

M_d (°C) = 413 – 13.7[Cr] – 9.5[Ni] -8.1[Mn] – 18.5[Mo] – 9.2[Si] – 462[C+N]

Eichelman & Hull (1953)

M_s (°C) = 1302 – 42[Cr] – 61[Ni] – 33[Mn] – 28 [Si] – 1667[C+N]

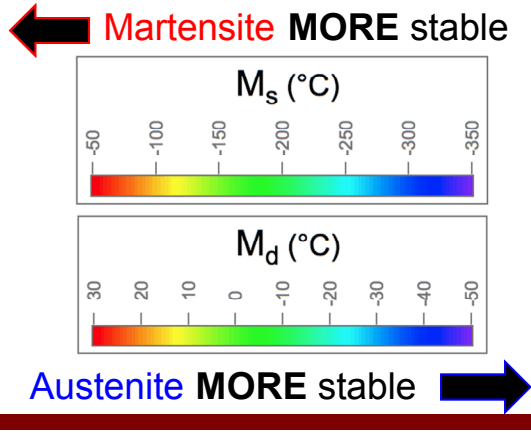

Ongoing work

- High throughput measurements of bcc-fraction
- FIB/TKD characterization of preparation-induced martensite depth
- Continued evaluation of electropolishing efficacy

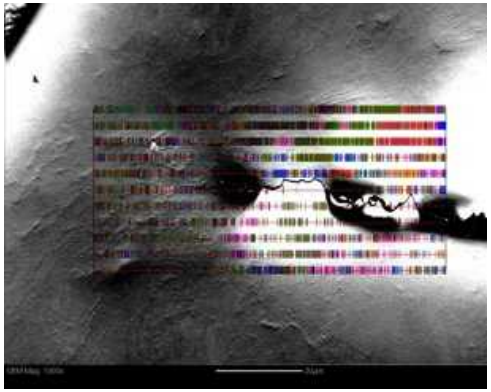

High-resolution EBSD line scan

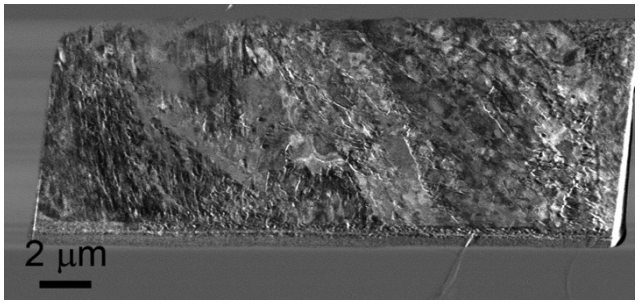

FIB lift-out for TKD

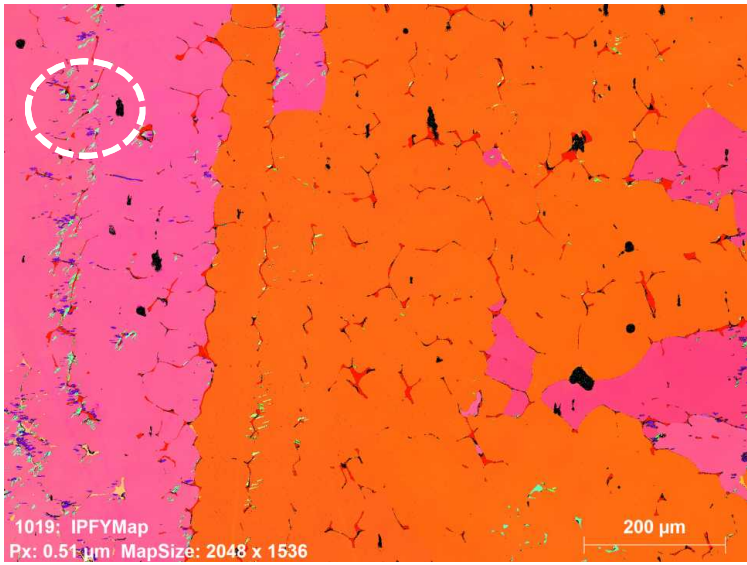

Electropolished CF8

Conclusions

- Deformation-induced martensite in austenitic stainless steel welds can result in misleading ferrite content measurements
- For unambiguous determination of ferrite content via EBSD, electropolishing is required
- Shear strain, irrespective of global loading condition, can promote room temperature martensite in 304/304L compositions
- Solute segregation during solidification locally increases propensity to form deformation-induced martensite

Acknowledgments

- The work has been funded wholly by DOE-NNSA Science Campaigns

- Special thanks to:
  - Charlie Robino
  - Alice Kilgo
  - Bonnie McKenzie
  - Dick Grant
  - Don Susan
  - Brad Salzbrenner
  - Corbett Battaile
  - Danny Maccallum

Sandia National Laboratories

Extra Slides

Deformation-Induced Martensite Dependent on Local Shear Strain Level Irrespective of Loading Condition

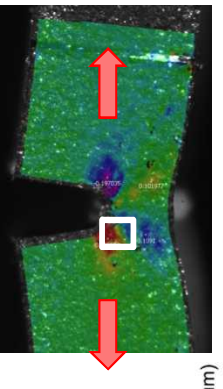

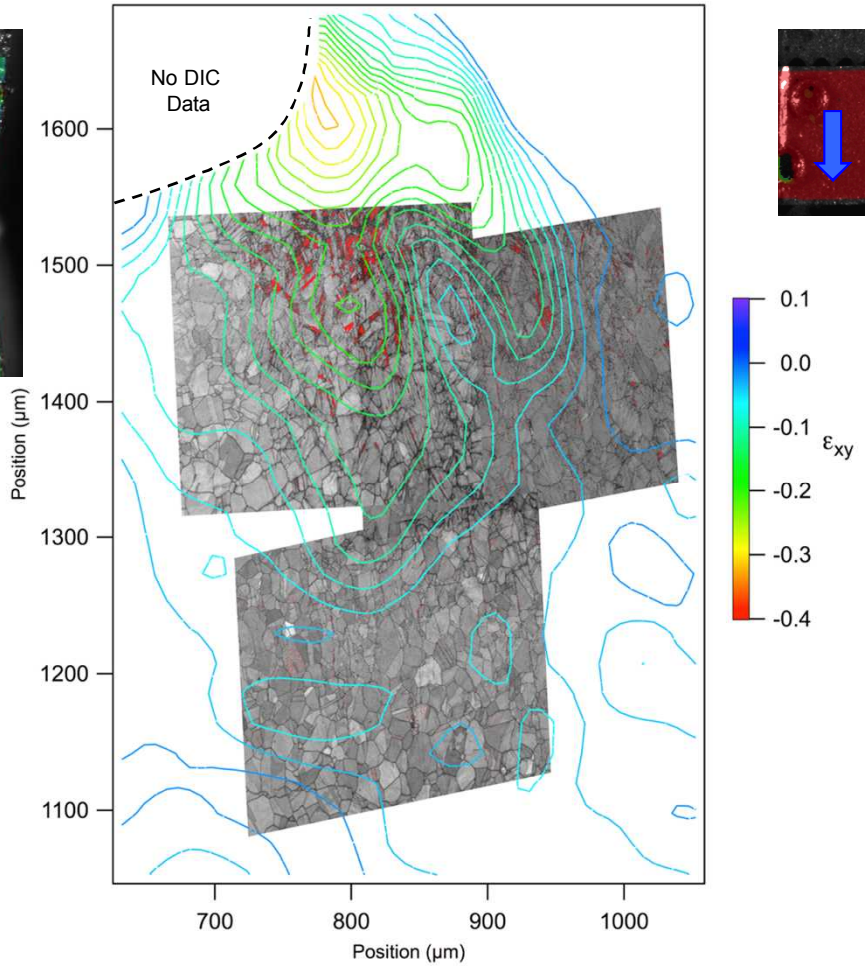

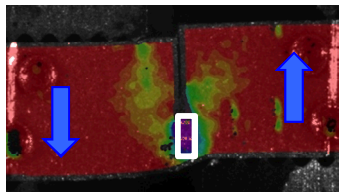

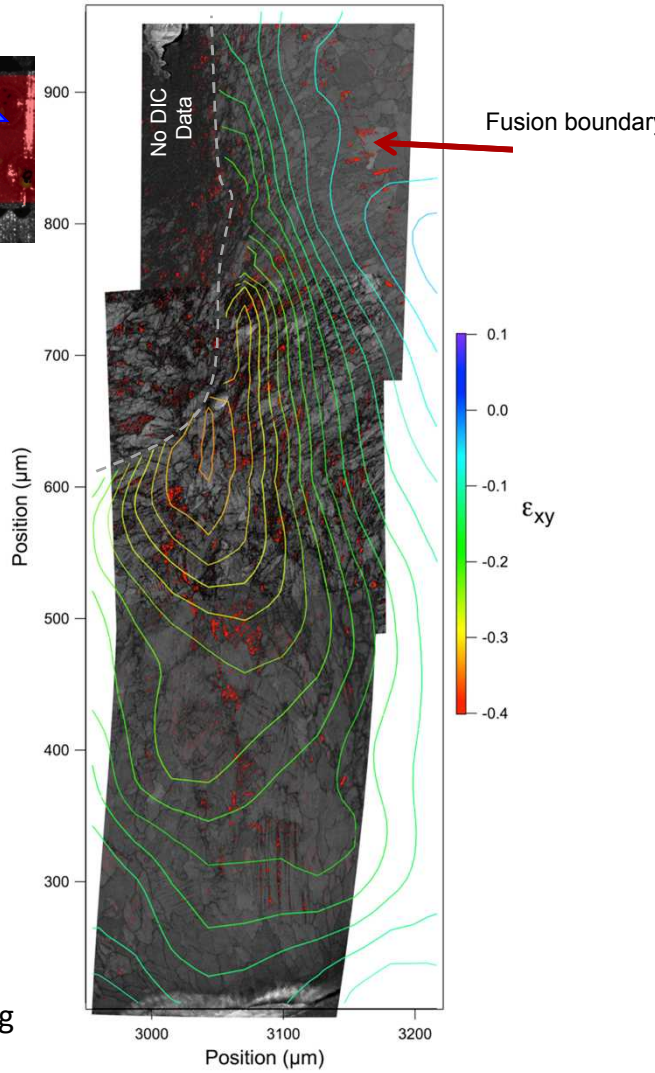

- Deformation-induced martensite dependent on local ε_{xy} level irrespective of loading condition
- Higher ε_{xy} magnitude resulting from shear loading likely leads to larger volume fraction
- Image correlation framework utilized for development of shear-strain dependent transformation model

EBSD suggests FCC to BCC Phase Change with Shear Loading

- Shear strain levels of ~50% resulted in deformed region with significant fraction of bcc-indexed phase

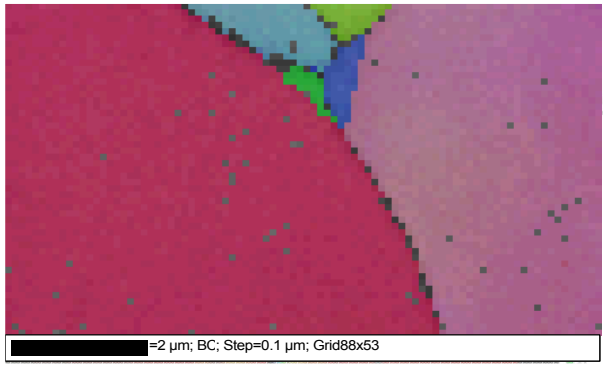

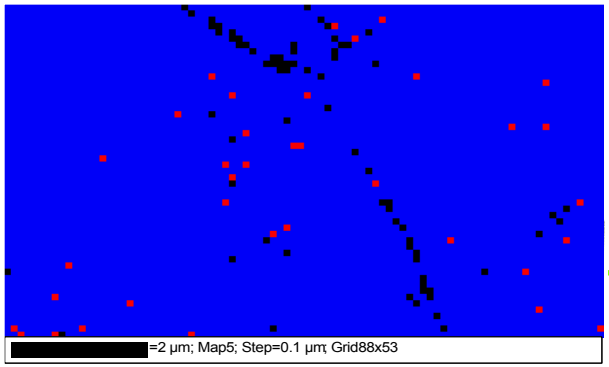

Away from fracture surface, scan area shows predominantly austenite

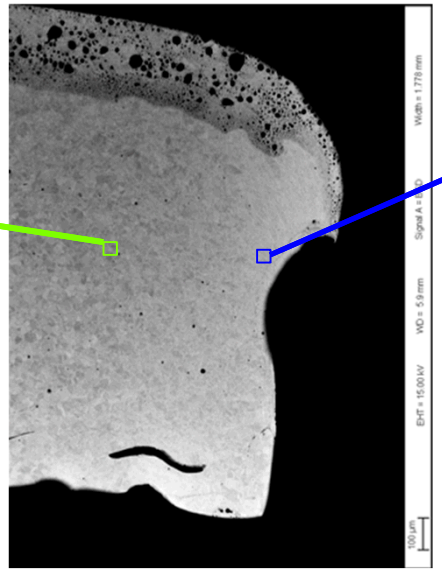

Sample electropolished after shear testing

Band Contrast

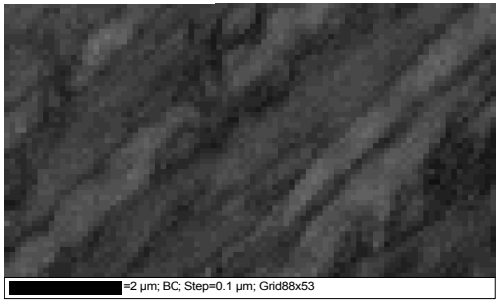

Phase Map: **bcc**; fcc

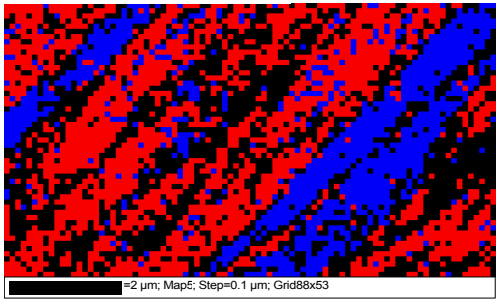

Inverse Pole Figure Map

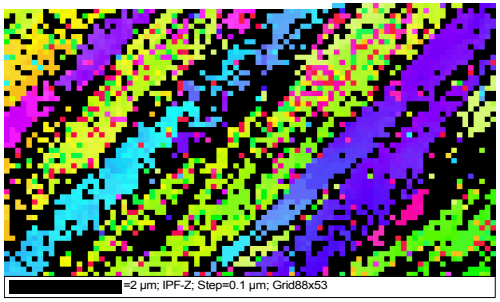

- EBSD problematic due to highly deformed shear region producing diffuse diffraction patterns

Transmission Kikuchi Diffraction Mapping using FIB-prepared specimens

- Recently-developed Transmission Kikuchi Diffraction (TKD) used to enable phase and orientation mapping of highly deformed, fine-scale bulk samples
- Spatial resolution significantly < 10nm

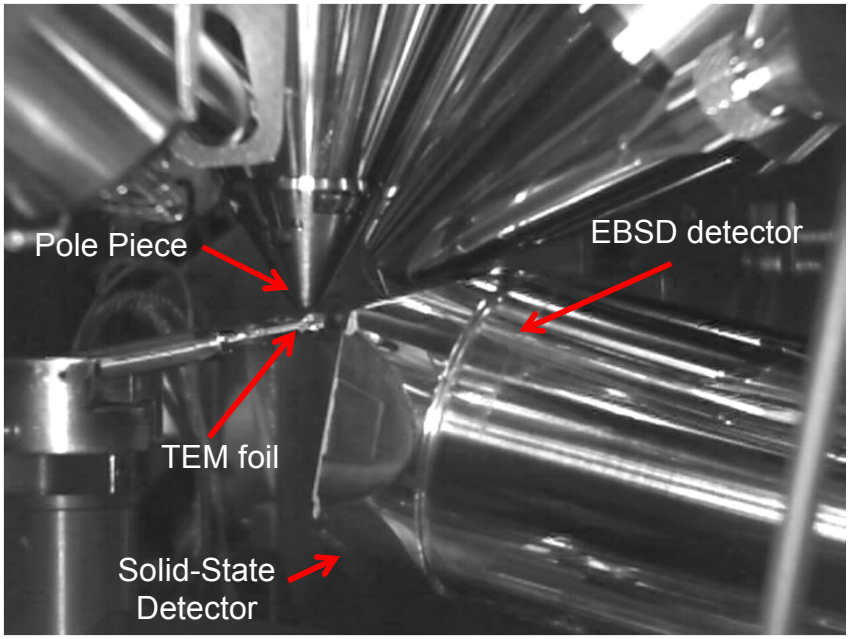

TKD setup in dual-beam FIB

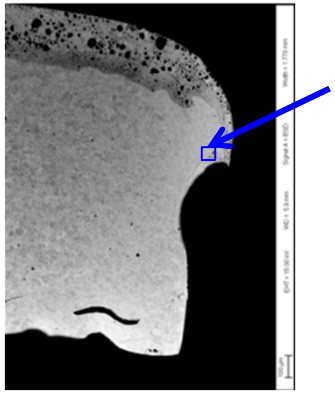

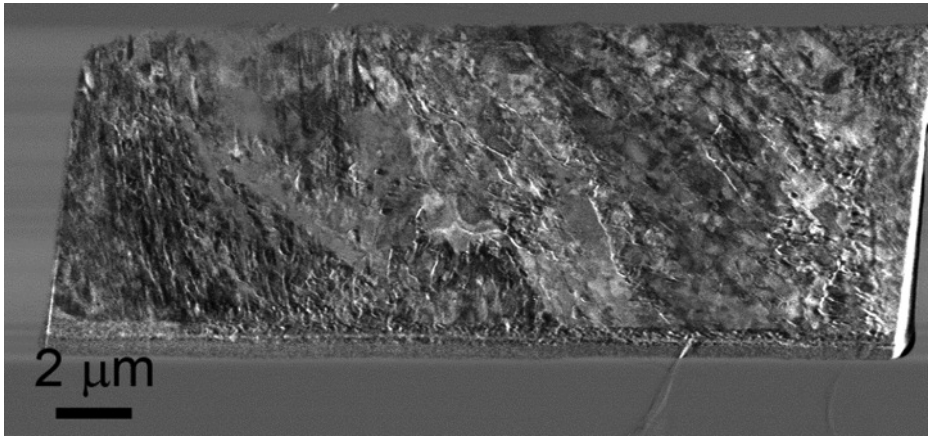

STEM image of FIB prepared 304L shear sample generated with SEM operated at 30 kV in transmission mode

FCC to BCC Phase Change Observed in Shear Loading

- Examined shear region predominantly indexed bcc
- Controlled shear loading test demonstrates austenite instability for a commercial 304L composition at room temperature
- A shear component to the deformation during polishing likely contributes to austenite instability
  - Can produce misleading information regarding δ-ferrite present in microstructure

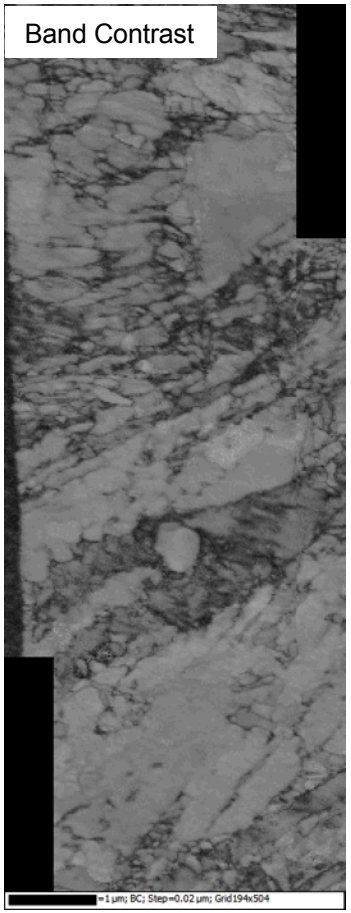

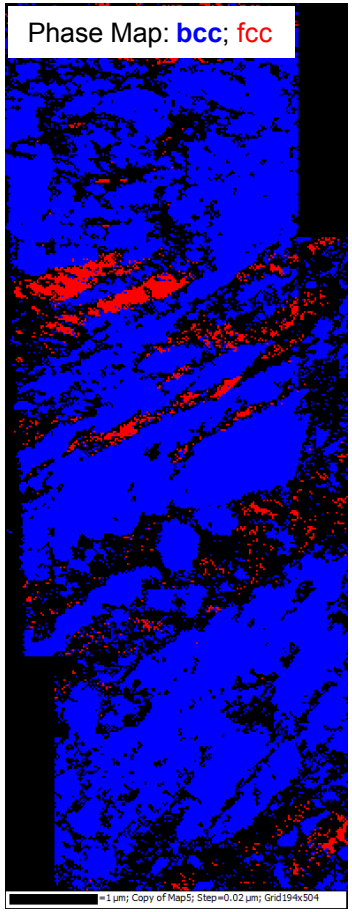

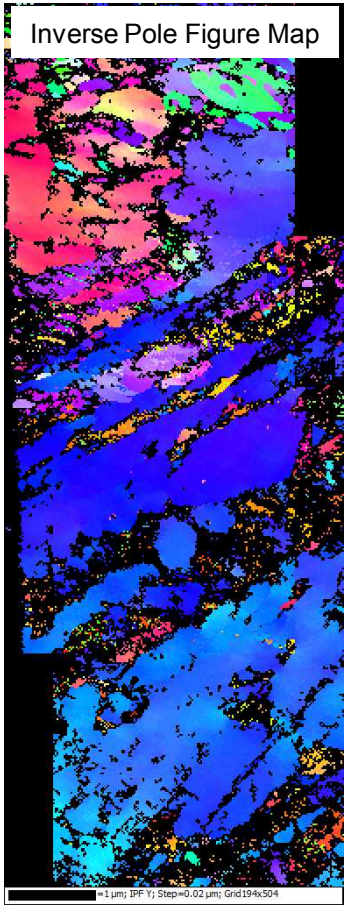

TKD Step Size: 20 nm